BMC Medical Imaging

RESEARCH

Open Access

Clinical value of the semi-quantitative parameters of ^{18}F-fluorodeoxyglucose PET/CT in the classification of hepatic echinococcosis in the Qinghai Tibetan area of China

Zhihui Shen[1†], Yuan Wang[1†], Xin Chen[2], Sai Chou[3], Guanyun Wang[1], Yong Wang[4], Xiaodan Xu[1], Jiajin Liu[1] and Ruimin Wang[1*]

Abstract

Background To investigate the value of ^{18}F-fluorodeoxyglucose (FDG) positron emission tomography (PET)/computed tomography (CT) semi-quantitative parameters, including the lesion diameter, maximum standardized uptake value (SUVmax), maximum standardized uptake value corrected for lean body mass (SULmax), metabolic lesion volume (MLV), and total lesion glycolysis (TLG), for classifying hepatic echinococcosis.

Methods In total, 20 patients with 36 hepatic echinococcosis lesions were included in the study. Overall, these lesions were categorized as hepatic cystic echinococcosis (HCE) or hepatic alveolar echinococcosis (HAE) according to the pathological results. Multiple semi-parameters including the maximum diameter, SUVmax, SULmax, MLV, and TLG were measured to classify HCE and HAE compared with the pathological results. The receiver operator characteristic curve and area under the curve (AUC) of each quantitative parameter were calculated. The Mann–Whitney U test was used to compare data between the two groups.

Results In total, 12 cystic lesions and 24 alveolar lesions were identified after surgery. There were significant differences in SUV max, SUL max, MLV, and TLG between the HAE and HCE groups ($Z = -4.70, -4.77, -3.36$, and -4.23, respectively, all $P < 0.05$). There was no significant difference in the maximum lesion diameter between the two groups ($Z = -0.77$, $P > 0.05$). The best cutoffs of SUV max, SUL max, MLV, and TLG for the differential diagnosis of HAE and HCE were 2.09, 2.67, 27.12, and 18.79, respectively. The AUCs of the four parameters were 0.99, 0.99, 0.85, and 0.94, respectively. The sensitivities were 91.7%, 87.5%, 66.7%, and 85.6%, respectively, and the specificities were 90.1%, 91.7%, 83.3%, and 90.9%, respectively.

Conclusion ^{18}F-FDG PET/CT semi-quantitative parameters had significant clinical value in the diagnosis and pathological classification of hepatic echinococcosis and evaluation of clinical treatment.

Keywords Hepatic echinococcosis, PET/CT, Classification, Semi-quantitative parameters

†Zhihui Shen and Yuan Wang contributed equally to this work.

*Correspondence:
Ruimin Wang
wrm@yeah.net
Full list of author information is available at the end of the article

Introduction

Hepatic echinococcosis (HE) is an uncommon zoonotic ailment with severe implications, resulting from larval invasions by Echinococcus granulosus and E. multilocularis. While the primary organ at risk is the liver, its clinical presentation can deceive by resembling aggressive malignant tumors [1, 2]. Globally, the prevalence of HE is notably high in rural communities in China, accounting for approximately 91% of new cases annually [3]. Studies show that among 64 patients treated for infected HE, the postoperative mortality rate was 3.1% [4]. HE can lead to chronic liver damage and liver abscesses, and if untreated, the mortality rate for HE exceeds 90% [5]. Despite improvements in surgical interventions with advancements in techniques and staging criteria, the mortality and complication rates remain significant. Effective early diagnosis and treatment are crucial for improving patient outcomes. This condition has been chiefly reported in regions such as China, North America, and Central Europe within the Northern Hemisphere [6, 7]. Surprisingly, although its underlying pathology suggests a harmless parasitic infection, HE can extend its reach, affecting vital organs such as the lungs, kidneys, spleen, and even the brain [8, 9]. Diverse imaging techniques, like ultrasound, CT, and MRI, provide valuable insights for its diagnosis and classification [10, 11]. The growth patterns of the parasites, in particular, are evident in these imaging results. For instance, hepatic cystic echinococcosis (HCE) is marked by its circular cystic expansion, while the hepatic alveolar echinococcosis (HAE), given its delicate nature, demonstrates a dynamic growth pattern [2, 12]. The diagnostic approach for HE is multifaceted. Initial diagnosis leans on imaging results, elevating to a probable case if associated with specific serum antibodies to E. multilocularis in blood tests, and is confirmed upon pathological findings or identifying the parasite's nucleic acid in clinical specimens [13]. Timely detection is vital, with surgical removal of the lesion being the gold standard of treatment, as underscored by the WHO-IWGE guidelines [14]. For those ineligibles for surgery, prolonged treatment with benzimidazole compounds, especially albendazole, is the chosen path, even though their exact parasiticidal efficacy remains under investigation [15].

In 2003 [16], the World Health Organization Informal Working Group on Echinococcosis (WHO-IWGE) introduced a standardized ultrasound imaging classification, building upon H. A. Gharbi et al.'s original system1. This categorizes cystic echinococcosis into three primary phases: active (CE1 and CE2), transitional (CE3), and inactive (CE4 and CE5). For cysts not visible via ultrasound, alternative imaging methods like CT or MRI are utilized. While MRI excels in pinpointing the intrinsic features of cysts comparable to ultrasound for stages CE1 to CE4, its limitation lies in detailing certain attributes like calcification [17, 18].

The ^{18}F-fluorodeoxyglucose positron emission tomography (18F-FDG PET) stands out as an effective instrument for discerning the metabolic activity of HE lesions [19]. Commonly, ^{18}F-FDG PET/CT is employed for initial cancer staging, monitoring tumor evolution, and recurrence. Among the quantifiable metrics used, the standardized uptake value (SUV) is predominant, often normalized to body weight. Its counterpart, normalized to lean body mass, is the SUL [20]. Yet, SUVmax merely captures the peak value within a lesion, neglecting details on tumor volume or diversity. In contrast, three-dimensional metrics like metabolic lesion volume (MLV) and total lesion glycolysis (TLG) provide a comprehensive view, proving to be credible indicators in cancer prognosis and therapy efficacy assessments [21–23].

In recent years, with the rapid growth in the number of PET/CT systems installed, the status of ^{18}F-FDG PET/CT in tumor and nontumor diagnosis and treatment has been fully affirmed, but there are few reports on the clinical value of the ^{18}F-FDG PET/CT quantitative parameters SUV max, maximum standardized uptake corrected for lean body mass (SUL max), MLV, and TLG in the diagnosis and pathological classification of HE [20].

Methods

Patients

This study was approved by the Human Ethics Committee of the Chinese PLA General Hospital (Ethics Committee Approval code: 2007-029), and all the methods described adhered to the principles of the Declaration of Helsinki. Written informed consent was obtained from all patients prior to recruitment. Twenty patients with HE diagnosed in the Department of Hepatobiliary Surgery of our hospital from October 2019 to July 2021, including 11 males and 9 females aged 14–67 years (mean age, 37 ± 15 years), were enrolled. Three of the patients were children. The past-history of the patients included two cases of hepatitis, one case of tuberculosis, and five cases of postoperative recurrence (Table 1). All patients were hospitalized in the hydatid disease area of our hospital. The diagnosis was confirmed by clinical and surgical pathology. The objective was to investigate the clinical utility of the 18F-FDG PET/CT quantitative parameters SUV max, SUL max, MLV, and TLG in the diagnosis and pathological classification of HE.

PET/CT examination

All patients underwent ^{18}F-FDG PET/CT scans using the German Siemens Biograph 64 PET/CT system before surgery (Fig. 1). Before intravenous injection of ^{18}F-FDG

Table 1 Clinical data of 20 patients with HE in the Qinghai Tibetan area of China

Patient	Age	Sex	Nation	Habitation	Pastoral life history	Animal contact history	Eating raw meat habit	Number of lesions	Distant infection	Pathological classification
1	33	M	Han	Gansu	Yes	Yes	No	Three	No	HAE
2	43	F	Tibetans	Qinghai	Yes	No	Yes	Single	Yes	HAE
3	24	M	Tibetans	Qinghai	Yes	No	Yes	Single	No	HCE
4	43	F	Tibetans	Qinghai	No	No	No	Single	No	HCE
5	31	M	Tibetans	Qinghai	Yes	Yes	Yes	Single	No	HCE
6	37	M	Tibetans	Qinghai	Yes	Yes	Yes	Single	No	HCE
7	67	M	Tibetans	Gansu	Yes	No	Yes	Single	No	HCE
8	38	F	Tibetans	Gansu	Yes	Yes	Yes	Three	No	HCE
9	57	F	Han	Gansu	Yes	Yes	Yes	Single	Yes	HAE
10	17	F	Tibetans	Qinghai	No	Yes	No	Single	No	HAE
11	28	M	Tibetans	Qinghai	Yes	No	Yes	Three	Yes	HAE
12	25	F	Tibetans	Qinghai	Yes	Yes	Yes	Single	Yes	HAE
13	28	M	Tibetans	Qinghai	Yes	Yes	Yes	Three	Yes	HAE
14	49	F	Tibetans	Qinghai	Yes	No	Yes	Single	No	HAE
15	15	F	Han	Qinghai	Yes	Yes	No	Single	Yes	HAE
16	34	M	Tibetans	Qinghai	Yes	No	Yes	Three	No	HCE
17	14	M	Tibetans	Qinghai	Yes	Yes	Yes	Three	No	HAE
18	42	F	Tibetans	Qinghai	Yes	No	Yes	Single	No	HAE
19	60	M	Tibetans	Qinghai	Yes	Yes	No	Three	No	HCE
20	59	M	Tibetans	Gansu	No	No	Yes	Three	No	HAE

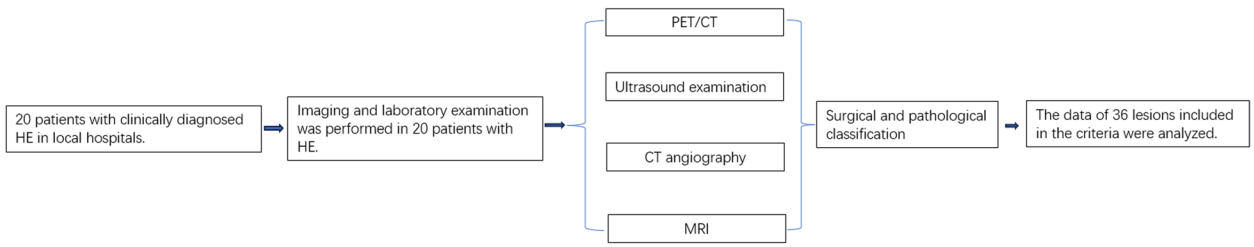

Fig. 1 Flowchart

(4.44–5.55 MBq/kg), patients are required to fast for 6 h and refrain from taking orally medications that may affect FDG intake. Blood glucose levels are < 11.1 mmol/L, and patients should rest in a quiet waiting room for at least 20 min. After 60 min of injection, images were collected from the skull base to the upper femur in free-breathing mode. CT parameters: current = 110 mAs, voltage = 120 kV, rotation = 0.5 s, layer thickness = 5 mm, and pitch = 1. The parameters of PET were 3-dimensional mode, the collection time was 2 min/ bed, 3 iterations, 21 subsets, 256 × 256 mm matrix, 5.0 mm FWHM [24]. The images were reconstructed with CT attenuation correction (AC) using the ordered subset expectation maximization algorithm (OSEM). There was a 3-day gap between the PET/CT scan and surgical excision.

Imaging data analysis

^{18}F-FDG PET/CT was performed in 20 patients with HE before surgery, and the imaging diagnosis was analyzed by two nuclear doctors, each with more than 5 years of experience in PET/CT diagnosis. First, the image quality was analyzed and judged by the blinding and visual method, and then the abnormal concentration of radioactivity in the whole body was observed. PET/CT images were analyzed using VB20A_HF08 software on the Syngo-Via workstation. A fixed threshold method (i.e., SUVmax of 2.5 or 40% of the highest SUVmax of the entire lesion) was used to determine tumor boundaries.

TLG was calculated as follows:

$$\mathrm{TLG} = \text{mean SUV (SUVmean)} \times \mathrm{MLV}.$$

SUL should preferably be calculated alongside SUV as follows:

$$\mathrm{SUL} = \mathrm{ActVOI\ (kBq/mL)/\ Actadministered\ (MBq)/LBM\ (kg)}.$$

Where ActVOI is the activity concentration measured in the volume of interest (VOI) and Actadministered is the net administered activity corrected for the physical decay of FDG to the start of acquisition and corrected for the residual activity in the syringe and/or administration lines and system.

$$\mathrm{LBM^M} = 9{,}270 \times \mathrm{weight}/(6{,}680 + 216 \times \mathrm{BMI})$$
$$\mathrm{LBM^F} = 9{,}270 \times \mathrm{weight}/(8{,}780 + 244 \times \mathrm{BMI})$$

Where LBMM and LBMF are the LBM for males and females, BMI is body mass index (weight/height2), and weight and height are in kilograms and meters, respectively.

Surgical and histopathology

After PET/CT examination, 20 HE patients underwent surgical treatment in the Department of General Surgery of our hospital. Then, it was sent to the pathology department, and each lesion was pathologically classified by an experienced pathologist.

Statistical analysis

The measurement data were expressed as the mean ± SD. SUVmax, SULmax, MLV, and TLG were compared between the groups using the Mann–Whitney U test, and the best cutoffs of SUVmax, SULmax, MLV, and TLG in the differential pathological classification of HE were determined by the receiver operating characteristic (ROC) curve. $P<0.05$ denoted statistical significance. All analyses were performed using the SPSS 22.0 statistical software package (IBM Analytics, Armonk, NY, USA).

Results

PET/CT findings and pathological classification of HE

Among the 20 patients, 12 had single lesions, and 8 had multiple lesions. Of the total 36 lesions, 18 were located in the right lobe of the liver, 12 were located in the left lobe of the liver, 3 were located in the caudate lobe of the liver, and 3 were located in the junction of the left and right hepatic lobes. The maximum diameter of the largest lesion, which was located in the right liver lobe, was approximately 32.81 cm, and the largest diameter of the smallest lesion, which was located in the left liver lobe, was approximately 0.90 cm. Thus, the range of the maximum diameter was 0.90–32.81 cm, and the mean diameter was 9.55 ± 5.24 cm. The ranges (mean) of SUVmax, SULmax, MLV, and TLG were 0.18−−50.62 (7.32 ± 10.43), 0.12–12.17 (3.77 ± 3.25), 0.3–976.25 (133.43 ± 242.35), and 0.32–7618.28 (614.47 ± 371.74), respectively.

On PET/CT imaging, the 36 lesions included 8 cystic lesions, 19 solid lesions, and 9 cystic–solid lesions, and 22 lesions were calcified. The lesions were classified by pathology as cystic ($n=12$) or alveolar ($n=24$, Table 2, Fig. 2). Among the 20 patients, two had bilateral lung infection, three had lymph node infection, and one had intracranial infection. Among the 20 patients, distant infection was found in 6 patients with HAE, while no distant infection was found in HCE patients. We found that distant infection may be a unique qualitative feature in distinguishing HAE and HCE.

Comparison of the maximum diameter, SUVmax, SULmax, MLV, and TLG between the two groups

The maximum diameter, SUVmax, SULmax, MLV, and TLG of the 12 cystic lesions and 24 alveolar lesions were compared between the two groups by the Mann–Whitney U test. There were significant differences in SUVmax, SULmax, MLV, and TLG between the two groups. However, the maximum lesion diameter did not differ between the groups (Table 3, Fig. 3).

ROC curve analysis

According to the ROC curve, SUVmax, SULmax, MLV and TLG showed good sensitivity and specificity for the differential diagnosis of HAE and HCE. (Table 4; Fig. 4).

Discussion

Echinococcosis, often manifested in the liver, arises from the larvae of E. multilocularis and E. granulosus infections [1]. The two primary forms of this disease are alveolar and cystic, linked to E. multilocularis and E. granulosus respectively. HAE, dubbed as "worm cancer", is a rarer, liver-affecting condition [6, 25, 26]. It presents a more aggressive progression compared to HCE. Notably, there's been an alarming growth in early HAE detections

Table 2 Differences in metabolic parameters in hepatic echinococcosis (mean ± SD)

Type	Number of lesions	Maximum diameter of lesion (cm)	SUVmax	SULmax	MLV	TLG
HAE	24	9.97 ± 8.15	10.61 ± 11.45	5.41 ± 2.74	194.73 ± 278.46	918.12 ± 1604.56
HCE	12	15.63 ± 22.19	0.72 ± 0.71	0.49 ± 0.53	10.81 ± 12.23	7.16 ± 18.13

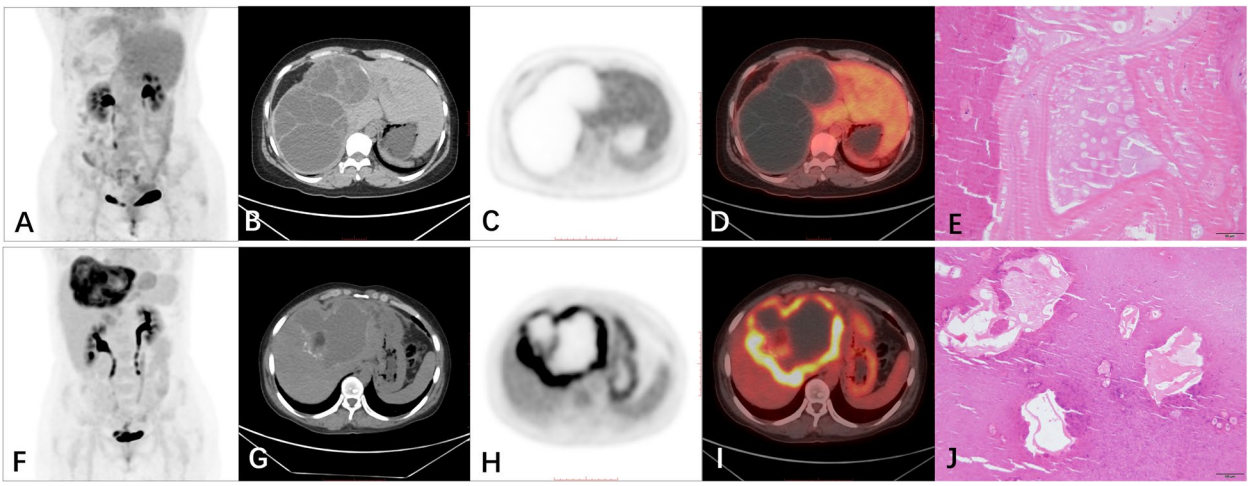

Fig. 2 **A**-**E** Representative ^{18}F-FDG PET/CT images of one patient with HCE (**A** maximum intensity projection (MIP), **B** CT, **C** PET, **D** fusion, **E** pathology). **F**, **J** Representative ^{18}F-FDG PET/CT images of one patient with HAE (**F** MIP, **G** CT, **H** PET, **I** fusion, **J** pathology)

Table 3 Comparison of quantitative parameters between the two groups

Parameters	SUVmax	SULmax	MLV	TLG	Maximum diameter of lesion
Z-scores	-4.70	4.77	3.36	-4.23	-0.77
P values	$P<0.001$	$P<0.001$	$P<0.001$	$P<0.001$	$P>0.001$

despite healthcare enhancements in China's western pastoral areas [27, 28]. Both these diseases are significant public health concerns, with HAE being among the deadliest helminthic infections.

Although HAE and HCE originate from the same family, their imaging results vastly differ. HCE is distinguished by its concentric growth, resulting in a round cystic lesion, enveloped by a protective stratified layer enclosing the parasite growth inside the germinal membrane. On the other hand, the delicate germinal membrane of HAE lacks such a protective layer [26, 29]. The growth of HAE is marked by the peripheral expansion of the metacestode within a granulomatous structure filled with macrophages, lymphocytes, fibroblasts, and neovessels, leading to higher FDG uptake [30]. Of the 36 studied lesions, there were a mix of cystic, solid, and combined types. A notable observation was the presence of calcification, appearing as eggshell-like or dispersed patterns. This is attributed to the erosion process of the liver tissue by HE lesions [31]. As the disease advances, these calcifications evolve into flocculent or irregular large foci [32], with larger lesions sometimes exhibiting ischemic necrosis and liquefaction [26]. HCE lesions typically display as round cystic masses, occasionally accompanied by gas or calcification.Although there are scarce reports on HCE in the literature and no differentiation between HCE and HAE, our findings highlight significant differences in SUVmax, SULmax, MLV, and TLG between HCE and HAE, emphasizing the clinical value of these semi-quantitative parameters in diagnosing and classifying hepatic echinococcosis.

For liver imaging, Ultrasound (US) stands as the primary choice, being non-invasive, cost-effective, and widely available [33–35]. However, when US fails to detect finer details, CT and MRI are instrumental. CT, more accessible in endemic regions than MRI, is adept at confirming calcifications and the nature of central necrosis [10]. MRI, meanwhile, is invaluable in detecting microcysts, hallmark indicators of AE [34].

At present, PET/CT is widely used in the evaluation of lesion stage, treatment response, and prognosis [36]. ^{18}F-FDG is the most commonly used PET/CT imaging agent at present. When glucose metabolism is abnormally increased, the ^{18}F-FDG intake of malignant tumors is significantly increased because malignant tumor cells are affected by local hypoxia, and some changes arise in tumor biological behavior. ^{18}F-FDG intake increases as the degree of malignancy of tumor cells and the rate of cell proliferation increase [37]. PET/CT has good consistency between the liquefaction state of the lesion edge and the proliferation state of the lesion, and it can reflect the biological activity characteristics of the lesion as well as its edge tissue cells [38]. This study found that HAE had more proliferating tissues at the edge of the lesion, faster cell proliferation, greater ^{18}F-FDG uptake by the proliferating tissues of the lesion, and a higher mean SUVmax than CE. Various parameters obtained by PET/CT,

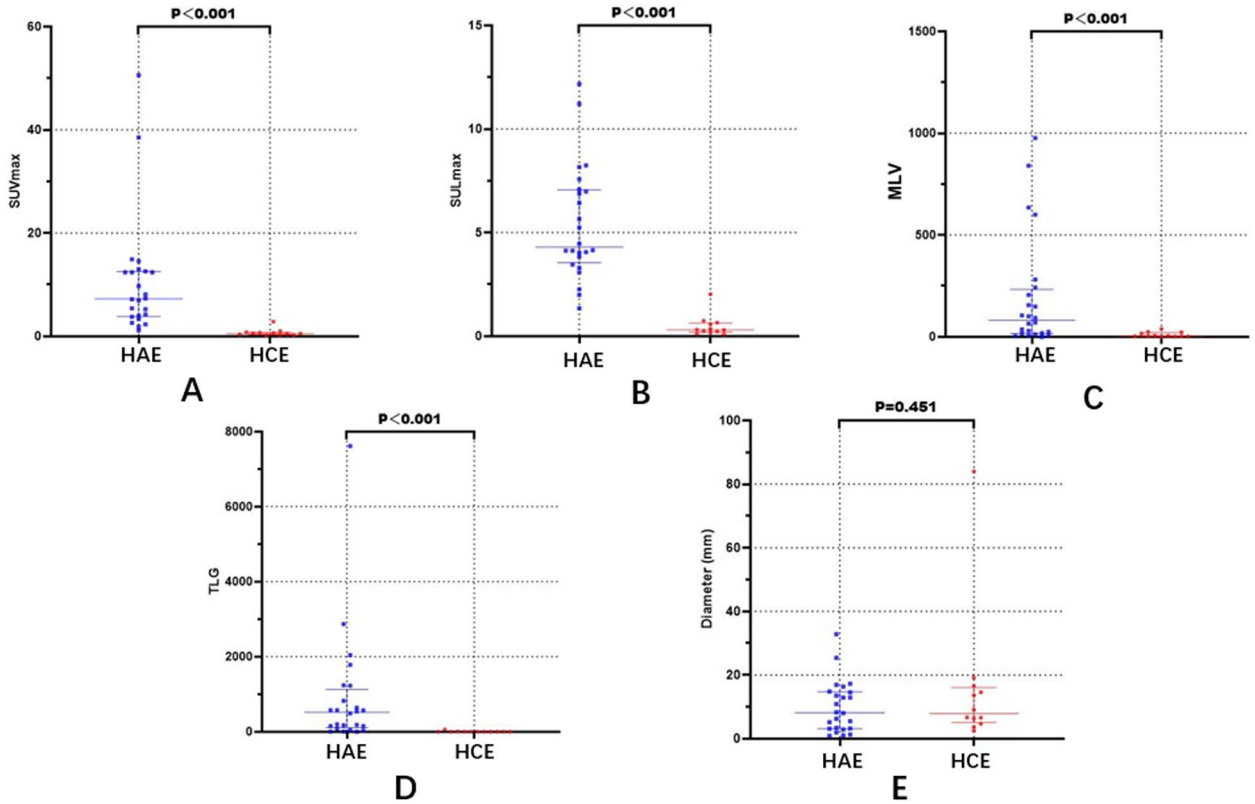

Fig. 3 Comparison of the maximum diameter (cm), SUVmax, SULmax, MLV, and TLG between the two groups. **A** Chart presents the results for SUVmax. **B** Chart presents the results for SULmax. **C** Chart presents the results for MLV. **D** Chart presents the results for TLG. **E** Chart presents the results for the maximum diameters (cm)

Table 4 Comparison of quantitative parameters for the differential diagnosis of HAE and HCE

Parameters	Cutoff	AUC (95%CI)	Sensitivity (%)	Specificity (%)
SUVmax	2.09	0.986 (0.965–0.989)	91.7	90.1
SULmax	2.67	0.993 (0.975–1.000)	87.5	91.7
MLV	27.12	0.847 (0.722–0.973)	66.7	83.3
TLG	18.79	0.938 (0.851–1.000)	85.6	90.9

including SUVmax and SULmax, reflect the proliferation degree of tumor cells. MLV reflects the lesion volume with high glucose metabolism, and TLG is the product of MLV and SUVmean in the lesion and a representation of the lesion load. SUVmax has become the most commonly used index for evaluating the metabolic activity of tumor cells because of its high convenience and repeatability. However, SUVmax is affected by many factors (blood glucose level, blood flow of the lesions, injection dose of the imaging agent, and attenuation correction of the instrument), and its prognostic value remains controversial. SULmax is the maximum standard intake value of patients with standardized LBM, and it is less affected by variables than SUVmax. Therefore, this study investigated the clinical value of multiple semi-quantitative parameters of PET/CT in the diagnosis of HE.

In the realm of ^{18}F-FDG PET/CT imaging, SUVmax serves as a prevalent semi-quantitative measure indicating disease intensity. However, its limitation lies in its focus on only the area of highest metabolic activity, sidelining the tumor's comprehensive metabolism or the complete tumor load. Alternatively, metabolic parameters like MLV and TLG, informed by FDG uptake and tumor volume, emerge as potential superior indicators with prognostic relevance1. As MLV amplifies, the concentration of clonogenic cells in the

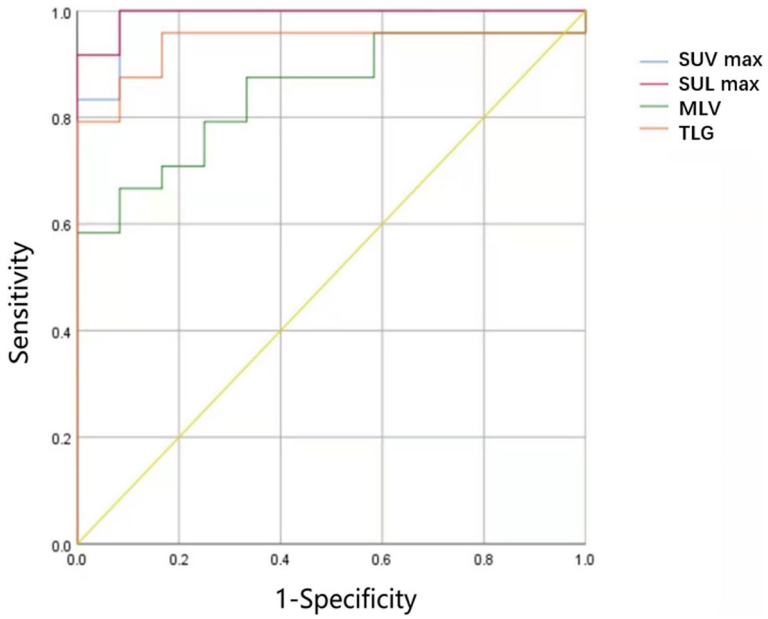

Fig. 4 ROC curve analysis for SUVmax, SULmax, MLV, and TLG

tumor escalates [39]. Concurrently, an elevation in TLG denotes heightened glucose metabolism within the lesion.Our research contrasted parameters, including SUVmax, SULmax, MLV, TLG, and maximum diameter, across 12 cystic and 24 vesicular lesions. It was found that while the maximum diameter showcased no variance, other parameters like SUVmax, SULmax, MLV, and TLG exhibited significant differences between the two groups. Interestingly, scant literature exists discussing these PET/CT quantitative metrics in the context of HCE and HAE differentiation. Our findings spotlight the prowess of SUVmax, SULmax, MLV, and TLG in distinguishing HCE from HAE with appreciable sensitivity and specificity. Although SUVmax and SULmax gauge tumor cell proliferation, they don't capture the complete tumor load, underscoring their constraints. Recent research attention has tilted towards novel PET/CT metabolic metrics such as MLV and TLG. These indicators offer a more holistic insight into lesion metabolic activity and volume, aligning better with PET's principle and the concept of tumor load. HAE lesions manifest a "proliferative infiltrating zone" replete with granulomas and neovascularization [40]. This zone is teeming with macrophages, lymphocytes, and fibroblasts. In stark contrast, HCE lesions, safeguarded by the germinal layer, remain non-invasive to adjacent parenchyma, devoid of granulomas or neovascularization [15]. This results in HAE lesions registering higher FDG uptakes. Reuter and colleagues [19] probed the metabolic activity dynamics in HAE's marginal zone using PET. Their observations highlight the relationship between lesion's proliferative infiltration zone and its specific developmental trajectory. Therefore, metrics like SUVmax and SULmax in the lesion's proliferation and infiltration zones could potentially be pivotal in evaluating HE treatment effectiveness. In the evolving landscape of medical imaging, PET/MRI emerges as a significant addendum to PET/CT. While PET/CT retains its dominant stature in oncology, the superior soft-tissue contrast offered by MRI might enhance the diagnostic process for specific malignancies. Additionally, a marked reduction in radiation exposure, especially beneficial for young adults and pediatric patients needing recurrent PET scans (as in lymphomas), solidifies the value proposition of PET/MRI [41, 42].

Some potential limitations of this study must be considered. First, the number of patients in our study was relatively small because HE is a rare disease. Moreover, the sample size of this study was small, which might have affected the cutoffs of the measured parameters. We need to further expand the sample size and conduct multicenter research to improve the clinical utility of semi-quantitative PET/CT parameters in the diagnosis and classification of HE.

Conclusion

The ^{18}F-FDG PET/CT quantitative parameters SUVmax, SULmax, MLV, and TLG have important clinical significance for the diagnosis, clinical classification and treatment response evaluation of HE.

Acknowledgements
Not applicable.

Authors' contributions
Conceptualization, Z.S. and R.W.; methodology, Y.W (Yuan Wang).; validation, X.C.; formal analysis, G.W.; investigation, Y.W (Yuan Wang). Y.W (Yong Wang). J.L. and X.X.; data curation, S.C.; writing—original draft preparation, Z.S.; supervision, R.W.; project administration, R.W. All authors have read and agreed to the published version of the manuscript.

Funding
This research received no external funding.

Availability of data and materials
The data presented in this study are available on request from the corresponding author. The data are not publicly available due to privacy regulations regarding patients.

Declarations

Ethics approval and consent to participate
This study was approved by the Human Ethics Committee of the Chinese PLA General Hospital. (Ethics Committee Approval code: 2007-029). This study was conducted in accordance with the Declaration of Helsinki. Informed consent was obtained from all the participants and their legal guardians.

Consent for publication
The informed consent for publication was obtained from the participants and their legal guardian.

Competing interests
The authors declare no competing interests.

Author details
[1]Department of Nuclear Medicine, The First Medical Centre, Chinese PLA General Hospital, No. 28 Fuxing Road, Beijing 100853, China. [2]Department of Pathology, The First Medical Centre, Chinese PLA General Hospital, No. 28 Fuxing Road, Beijing 100853, China. [3]Department of General Surgery, The First Medical Centre, Chinese PLA General Hospital, No. 28 Fuxing Road, Beijing 100853, China. [4]Department of Nuclear Medicine, The Fifth Medical Center, Chinese PLA General Hospital, No. 8, Dongdajie Street, Fengtai District, Beijing 100071, China.

Received: 7 September 2023 Accepted: 18 July 2024
Published online: 31 July 2024

References

1. McManus DP, Zhang W, Li J, et al. Echinococcosis. Lancet. 2003;362(9392):1295–304.
2. Kern P, Menezes da Silva A, Akhan O, et al. The Echinococcoses: diagnosis, clinical management and burden of disease. Adv Parasitol. 2017;96:259–369.
3. Torgerson PR, Keller K, Magnotta M, et al. The global burden of alveolar echinococcosis. PLoS Negl Trop Dis. 2010;4(6):e722.
4. Manterola C, Urrutia S, MINCIR GROUP. Infected hepatic echinococcosis: results of surgical treatment of a consecutive series of patients. Surg Infect (Larchmt). 2015;16(5):553–7.
5. Gottstein B, Wittwer M, Schild M, et al. Hepatic gene expression profile in mice perorally infected with Echinococcus multilocularis eggs. PLoS One. 2010;5(4):e9779.
6. Wen H, Vuitton L, Tuxun T, et al. Echinococcosis: advances in the 21st century. Clin Microbiol Rev. 2019;32(2):e00075–e118.
7. Solange B-H, Laurent S, Francois C. Hepatic alveolar echinococcosis. Semin Liver Dis. 2021;41(3):393–408.
8. Schwarze V, Mueller-Peltzer K, Negrão de Figueiredo G, et al. The use of contrast-enhanced ultrasound (CEUS) for the diagnostic evaluation of hepatic echinococcosis. Clin Hemorheol Microcirc. 2018;70(4):499–455.
9. Kratzer W, Gruener B, Kaltenbach TE, et al. Proposal of an ultrasonographic classification for hepatic alveolar echinococcosis: Echinococcosis multilocularis Ulm classification-ultrasound. World J Gastroenterol. 2015;21(43):12392–402.
10. Graeter T, Kratzer W, Oeztuerk S, et al. Proposal of a computed tomography classification for hepatic alveolar echinococcosis. World J Gastroenterol. 2016;22(13):3621–31.
11. Greco S, Cannella R, Giambelluca D, et al. Complications of hepatic echinococcosis: multimodality imaging approach. Insights Imaging. 2019;10(1):113.
12. Calame P, Weck M, Busse-Cote A, et al. Role of the radiologist in the diagnosis and management of the two forms of hepatic echinococcosis. Insights Imaging. 2022;13(1):68.
13. Brumpt E, Blagosklonov O, Calame P, et al. AE hepatic lesions: correlation between calcifications at CT and FDG-PET/CT metabolic activity. Infection. 2019;47(6):955–60.
14. Brunetti E, Kern P, Vuitton DA. Writing Panel for the WHO IWGE Expert consensus for the diagnosis and treatment of cystic and alveolar echinococcosis in humans. Acta Trop. 2010;114(1):1–16.
15. Ammann RW, Stumpe KD, Grimm F, et al. Outcome after discon tinuing long-term benzimidazole treatment in 11 patients with nonresectable Alveolar Echinococcosis with negative FDG PET/CT and Anti-EmII/3-10 Serology. PLoS Negl Trop Dis. 2015;9(9):e0003964.
16. WHO Informal Working Group. International classification of ultrasound images in cystic echinococcosis for application in clinical and field epidemiological settings. Acta Trop. 2003;85(2):253–61.
17. AgudeloHiguita NI, Brunetti E, McCloskey C. Cystic echinococcosis. J Clin Microbiol. 2016;54(3):518–23.
18. Botezatu C, Mastalier B, Patrascu T. Hepatic hydatid cyst-diagnose and treatment algorithm. J Med Life. 2018;11(3):203–9.
19. Reuter S, Grüner B, Buck AK, et al. Long-term follow-up of metabolic activity in human alveolar echinococcosis using FDG-PET. Nuklearmedizin. 2008;47(4):147–52.
20. Boellaard R, Delgado-Bolton R, Oyen WJ, et al. FDG PET/CT: EANM procedure guidelines for tumor imaging: version 2.0. Eur J Nucl Med Mol Imaging. 2015;42(2):328–54.
21. Ayako K, Yuji N, Takayoshi I, et al. Prognostic value of quantitative parameters of ^{18}F-FDG PET/CT for patients with angiosarcoma. AJR Am J Roentgenol. 2020;214(3):649–57.
22. Liao S, Penney BC, Wroblewski K, et al. Prognostic value of metabolic tumor burden on ^{18}F-FDG PET in nonsurgical patients with non-small cell lung cancer. Eur J Nucl Med Mol Imaging. 2012;39(1):27–38.
23. Kim CY, Hong CM, Kim DH, et al. Prognostic value of whole-body metabolic tumor volume and total lesion glycolysis measured on ^{18}F-FDG PET/CT in patients with extranodal NK/T-cell lymphoma. Eur J Nucl Med Mol Imaging. 2013;40(9):1321–9.
24. Shen Z, Wang R. Comparison of 18F-FDG PET/CT and 68Ga-FAPI in spindle cell rhabdomyosarcoma. Diagnostics (Basel). 2023;13(18):3006.
25. Bo R, Jian W, Zhoulin M, et al. Hepatic alveolar echinococcosis: predictive biological activity based on radiomics of MRI. Biomed Res Int. 2021;2021:6681092.
26. Bulakçı M, Kartal MG, Yılmaz S, et al. Multimodality imaging in diagnosis and management of alveolar echinococcosis: an update. Diagn Interv Radiol. 2016;22(3):247–56.
27. Feng X, Qi X, Yang L, et al. Human cystic and alveolar echinococcosis in the Tibet Autonomous Region (TAR), China. J Helminthol. 2015;89(6):671–9.
28. Wang X, Dai G, Li M, et al. Prevalence of human alveolar echinococcosis in China: a systematic review and meta-analysis. BMC Public Health. 2020;20(1):1105.
29. Eckert J, Deplazes P. Biological, epidemiological, and clinical aspects of echinococcosis, a zoonosis of increasing concern. Clin Microbiol Rev. 2004;17(1):107–35.
30. Bresson-Hadni S, Delabrousse E, Blagosklonov O, et al. Imaging aspects and non-surgical interventional treatment in human alveolar echinococcosis. Parasitol Int. 2006;55(Suppl):S267–272.
31. Cai DW, Wang HY, Wang XL, et al. Ultrasonographic fingings of small lesion of hepatic alveolar echinococcosis. Acta Trop. 2017;174:165–70.
32. Gottstein B, Soboslay P, Ortona E, et al. Immunology of alveolar and cystic echinococcosis (AE and CE). Adv Parasitol. 2017;96:1–54.

33. Liu W, Delabrousse É, Blagosklonov O, et al. Innovation in hepatic alveo lar echinococcosis imaging: best use of old tools, and necessary evaluation of new ones. Parasite. 2014;21:74.
34. Bartholomot G, Vuitton DA, Harraga S, et al. Combined ultrasound and serologic screening for hepatic alveolar echinococcosis in central China. Am J Trop Med Hyg. 2002;66(1):23–9.
35. Kantarci M, Bayraktutan U, Karabulut N, et al. Alveolar echinococcosis: spectrum of findings at cross-sectional imaging. Radiographics. 2012;32(7):2053–70.
36. Mikhaeel NG, Smith D, Dunn JT, et al. Combination of baseline metabolic tumor volume and early response on PET/CT improves progression-free survival prediction in DLBCL. Eur J Nucl Med Mol Imaging. 2016;43(7):1209–19.
37. Zheng JJ, Wang J, Zhao JQ, et al. Diffusion-weighted MRI for the initial viability evaluation of parasites in hepatic alveolar echinococcosis: comparison with positron emission tomography. Korean J Radiol. 2018;19(1):40–6.
38. Abulaihaiti M, Wu XW, Qiao L, et al. Efficacy of albendazolechitosan microsphere-based treatment for alveolar echinococcosis in mice. PLoS Neglect Trop D. 2015;9(9):15–6.
39. Martínez A, Infante J R, Quirós J, et al. Baseline (18)F-FDG PET/CT quantitative parameters as prognostic factors in esophageal squamous cell cancer. Rev Esp Med Nucl Imagen Mol (Engl Ed). 2022;41(3):164–70.
40. Caoduro C, Porot C, Vuitton DA, et al. The role of delayed 18F-FDG PET imaging in the follow-up of patients with alveolar echinococcosis. J Nucl Med. 2013;54(3):358–63.
41. Martin O, Schaarschmidt BM, Kirchner J, et al. PET/MRI versus PET/CT for whole-body staging: results from a single-center observational study on 1,003 sequential examinations. J Nucl Med. 2020;61(8):1131–6.
42. Lötsch F, Waneck F, Groger M, et al. FDG-PET/MRI imaging for the management of alveolar echinococcosis: initial clinical experience at a reference centre in Austria. Trop Med Int Health. 2019;24(6):663–70.

Publisher's Note